Catal Lett (2017) 147:1061–1076
DOI 10.1007/s10562-017-1993-9

CuO Nanoparticle Immobilised Mesoporous TiO_2–Cobalt Ferrite Nanocatalyst: A Versatile, Magnetically Separable and Reusable Catalyst

Barun Kumar Ghosh[1] · Debabrata Moitra[1] · Madhurya Chandel[1] · Manoj Kumar Patra[2] · Sampat Raj Vadera[2] · Narendra Nath Ghosh[1]

Received: 15 December 2016 / Accepted: 6 February 2017 / Published online: 23 February 2017

Abstract Here, synthesis and catalytic activity of a novel nanocatalyst ($CuO@mTiO_2@CF$), consisting of CuO nanoparticles, mesoporous titanium oxide and Cobalt ferrite have been reported for the first time. The catalyst was synthesized using a simple aqueous solution based chemical methodology. Synthesized $CuO@mTiO_2@CF$ showed excellent catalytic activity towards various organic reactions such as (i) Epoxidation of styrene, (ii) Click reaction, (iii) Biginelli reaction, (iv) Reduction of 4-Nitrophenol and trifluralin in presence of excess $NaBH_4$. Moreover, this novel nanocatalyst offered easy magnetic separation after the catalysis reaction and excellent reusability. Easy synthesis methodology, versatility, good reusability and easy separation make the nanocatalyst attractive in the field of heterogeneous catalysis.

Graphical Abstract

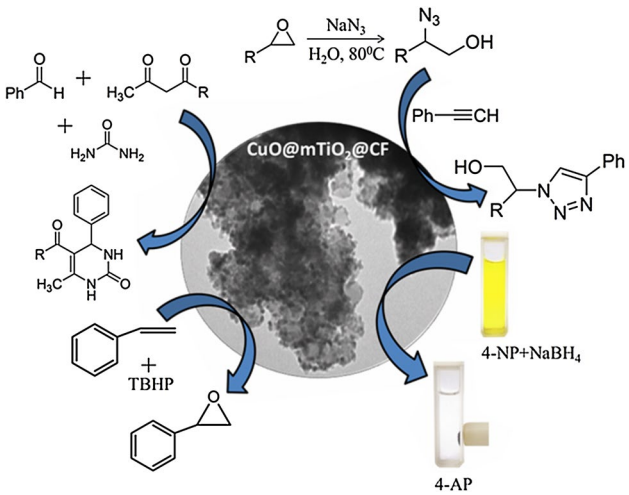

Keywords Magnetically separable catalyst · Styrene epoxidation · Biginelli reaction · Click reaction · 4-Nitrophenol reduction

1 Introduction

Recently, development of hybrid materials having multifunctional catalytical activity immerged as a vital research area to meet the demands of various pharmaceutical and fine chemical industries. Some of the important features which are expected from these new generation catalysts are (i) versatility: ability to act as catalyst for various types of organic reactions, (ii) high catalytic efficiency, (iii) easy recovery, (iv) good reusability, (v) environment friendliness etc. Keeping these points in mind, we have designed a catalyst composed of CuO, mesoporous TiO_2 and $CoFe_2O_4$

Electronic supplementary material The online version of this article (doi:10.1007/s10562-017-1993-9) contains supplementary material, which is available to authorized users.

✉ Narendra Nath Ghosh
naren70@yahoo.com

[1] Nanomaterials Lab, Department of Chemistry, Birla Institute of Technology and science, K. K. Birla Goa Campus, Zuarinagar, Pilani, Goa 403726, India

[2] Defence Lab, Jodhpur 342011, India

nanoparticles and investigated its catalytic activity towards (i) Epoxidation of styrene in presence of tert-Butyl hydroperoxide (TBHP), (ii) Biginelli reaction for synthesis of 3,4 dihydropyrimidinones (DHPMs) in solventless condition, (iii) 'Click reaction' for synthesis 1,2,3 triazole derivatives using in aqueous medium and (iv) reduction of 4-NP and a herbicide 'trifluralin' in presence of excess $NaBH_4$. We have chosen these reactions because of their high commercial, biological and environmental importance.

Due to wide range of applications of epoxides, such as useful and versatile intermediate for the synthesis of many pharmaceutical products, fine chemicals, commodities etc. [1–3], olefin epoxidation has gained immense interest over the last few years. Epoxidation of olefins is one of the main routes for the production of epoxides [3]. However, epoxidation of styrene is very difficult because of the presence of olefinic group in the terminal position [4]. Conventional procedure of epoxidation of styrene using peracids suffers from some disadvantages, like production of high amount of undesirable by-products, harsh reaction conditions, cost effectiveness etc [3, 4]. Hence, there is enormous interest in developing novel heterogeneous catalysts for epoxidation reactions. Examples of some reported catalysts are noble metal nanocatalyst, mesoporous silica or titanium based catalysts etc [1, 5–9]. Linares et al. reported colloidal Au immobilized on mesoporous silica as highly active and selective catalyst for styrene epoxidation using H_2O_2 [1]. Similar reaction was also investigated by Liu et al. using SiO_2–Au catalysts, synthesized via one-pot method [10]. Choudhary et al. utilized Au nanoparticles supported on Yb_2O_3 for styrene epoxidation [4]. Liu et al. reported gold Carbon Nanotube-supported gold catalysts for styrene epoxidation [11]. Studies on Ag doped catalysts (e.g. Ag–TiO_2, Fe_3O_4–Ag, CuO@Ag etc.) have also been reported [12–14]. In recent years, catalysts consisting of entirely non noble metal or metal oxides have been developed because of their high activity as well as low cost than noble precious metal based catalysts. For example, Zhang et al. reported an efficient Fe_3O_4–CuO@meso–SiO_2 magnetically recyclable catalyst for styrene epoxidation [8]. Thao et al. demonstrated the usefulness of Cu-doped hydrotalcites catalyst for styrene epoxidation [15]. Wang et al. prepared a series of metal ion doped TiO_2 nanoparticles having tunable catalytic activities for oxidation of organic compounds [3]. However, difficulty of recovering the catalysts after reactions, their reusability, complicated synthesis routes for the catalyst preparation still pose the major challenges.

Biginelli condensation involves one-pot multicomponent condensation of an aldehyde, ethyl acetoacetate and urea, for preparation of dihydropyrimidinone derivative [16]. Synthesis of DPHMs and derivatives are important because of their wide range pharmaceutical and therapeutic applications such as anti-inflammatory agents, calcium channel blockers, antihypertensive, anti-tumor, adrenergic and neuropeptide antagonists etc [16, 17]. As original Biginelli reaction suffers from some serious limitations (such as use of strong acidic catalyst, poor yield, etc. [18]) several improved procedures involving heterogeneous catalysts have been reported. For example, Fe_3O_4@SiO_2–imid–$H_3PMo_{12}O_{40}$ [17], Fe_3O_4@mesoporous SBA-15 [19], MnO_2–MWCNT [20], Acidic Choline-Based Ionic Liquids [21], sulfonated-phenylacetic acid coated Fe_3O_4 [22], cellulose sulfuric acid [23], nano ZnO [24], SiO_2–$CuCl_2$ [25], Nafion–Ga [26] etc. have been reported for Biginelli reaction. But, despite of the efforts made in recent years for Biginelli reaction, difficulty in catalyst recovery and complicated procedures for catalyst preparation remain as typical problems.

Synthesis of Triazoles by 'click reaction', introduced by Sharpless and co-workers [27], have received considerable interest because of the useful applications of triazoles as biologically active chemicals, agrochemicals, pharmaceuticals, drug molecules with significant anti-HIV activity, anti microbial activity against Gram positive bacteria etc [28]. Several authors have reported Cu based catalysts for the synthesis of triazole derivatives including Cu^{II}-hydrotalcite [28], mesoporous CuO [29], Copper(I)–Zeolite [30], 4′-Phenyl-2,2′:6′,2″-Terpyridine Copper(II) complex immobilized on activated multiwalled carbon nanotubes [31], $CuFe_2O_4$ nanoparticles [32], CuI [33], copper(I)@phosphorated SiO_2 [34], Copper nanoparticles on activated carbon [(NHC)CuCl] complex [35, 36], $CuSO_4{\cdot}5H_2O$ with a sodium ascorbate additive [37], Silica-immobilized NHC–Cu(I) [38], Polystyrene-supported ionic liquid copper complex [39] etc. However, in some cases the limitations which are associated with these procedures are elevated reaction temperature, formation of undesired products, low yields, use of homogeneous catalysts, harsh reaction conditions to synthesize the catalysts etc [28]. Moreover, use of magnetically separable catalysts for synthesis of β-hydroxy triazoles by employing epoxides as starting compounds and 1,3 dipolar cycloaddition are limited in literature.

Water pollution caused from the colored effluents discharged from various industries (such as plastics, paper and pulp manufacturing, dying of cloth, leather treatment, printing, etc.) is one of the major environmental concerns [40]. Strong color of these pollutants causes serious aesthetic and ecological problems to the receiving aquatic ecosystems, such as inhibition of benthic photosynthesis [41]. Among these pollutants, according to US Environmental Protection Agency, nitrophenols are one of the most hazardous due to their carcinogenic and genotoxic nature [42]. To address this issue, reduction of nitrophenols to environmentally benign colorless amines is an attractive strategy.

Another added advantage of this strategy is that formation of aminophenols as products, which are pharmaceutically important compounds and used as vital intermediate of many organic synthesis, anti-inflammatory agents, calcium channel blockers, anti-tumor, antihypertensive, adrenergic and neuropeptide antagonists etc [43–45]. Thus, transformation of 4-nitrophenol to 4-aminophenol is an environmentally as well as industrially important reaction. For this reaction, precious metal nanoparticle (Au, Ag, Pt, Pd etc.) based catalysts have been reported widely during last few years [46–57]. But the high cost of the precious metals limits their practical application [44, 58]. Recently, transition metal based catalysts have also reported for this reaction [44, 45, 58–62].

Though nanoparticles are expected to exhibit high catalytic activity due to high surface to volume ratio, but they tend to form agglomerates, which in turn reduce the access of the reactants to catalytically active sites and reduce their catalytic activity. Another limitation associated with nanosized catalyst is their separation from the reaction mixture after reaction, because simple filtration or centrifugation processes are not very efficient in this case. To address these issues, one of the common strategies is to immobilize the nanoparticles on the surface of solid supports. However, easy recovery of these catalysts for their regeneration is still a challenging issue. Recently, magnetic separation of catalysts from reaction mixture has become an attractive strategy for its easy but efficient separation.

2 Experimental

2.1 Materials Used

Cobalt nitrate ($Co(NO_3)_2{\cdot}6H_2O$), Iron nitrate ($Fe(NO_3)_3{\cdot}9H_2O$), Copper Nitrate ($Cu(NO_3)_2{\cdot}3H_2O$), Ethylenediaminetetraacetic acid (EDTA), Titanium chloride ($TiCl_3$), Urea, Cetyltrimethylammonium bromide (CTAB), Sodium azide (NaN_3) were purchased from Merck, India. Styrene, Styrene oxide, Cyclohexene, Cyclohexene oxide, TBHP (5–6 M in decane), Benzaldehyde, Phenylacetylene, Ethyl acetoacetate, Acetyl acetone, were purchased from Sigma-Aldrich. Commercial TiO_2 (Hombikat) was purchased from Fluka. All chemicals were used without further purification. Deionized water was used throughout the experiment.

2.2 Synthesis of Catalysts

To synthesize the catalyst composed of $CoFe_2O_4$, TiO_2 and CuO, we have first synthesized $CoFe_2O_4$ nanoparticles (CF). Then using these CF nanoparticles mesoporous TiO_2 ($mTiO_2$)–CF composite was prepared. Finally, on the porous surface of $mTiO_2$@CF, CuO nanoparticles were immobilized.

$CoFe_2O_4$ nanoparticles were synthesized using an aqueous solution based EDTA precursor method developed by us and reported elsewhere [63]. To synthesize $mTiO_2$@CF, 3.42 g of CTAB was dissolved in 20 ml water and 10 ml NH_4OH (30%) solution at 30 °C. To this solution, 10 ml aqueous dispersion containing 250 mg of $CoFe_2O_4$ was added with continuous mechanical stirring. Separately, in a beaker 9.67 g of $TiCl_3$ (15%) was oxidized by adding aqueous solution of HNO_3 dropwise until the solution became colorless. This solution was then dropwise added to $CoFe_2O_4$ dispersed CTAB solution with constant stirring. pH of the reaction mixture was maintained at 9/10 by adding aqueous NH_4OH or HNO_3. This solution was further stirred mechanically for 4 h at room temperature. The resulting mixture was then transferred to a Teflon bottle followed by aging for 24 h at 30 °C. The solid product thus formed was separated by filtration, washed with water and dried in oven at 100 °C for 12 h. The resulting material was calcined at 550 °C for 3 h to obtain $mTiO_2$@CF.

To prepare CuO nanoparticle loaded $mTiO_2$@CF, 0.450 g of $mTiO_2$@CF powder was mixed with 6 ml aqueous solution containing 0.141 mg $Cu(NO_3)_2.3H_2O$ and soaked for 6 h. The mixture was then dried on a hot plate. The powder thus obtained was then calcined at 550 °C for 3 h to obtain CuO nanoparticles loaded $mTiO_2$@CF (CuO@$mTiO_2$@CF).

2.3 Catalytic Activity Study

2.3.1 Epoxidation of Styrene

A mixture of styrene (5 mmol, 0.575 ml), acetonitrile (4 ml) and the catalyst (50 mg, CuO@$mTiO_2$@CF) was first taken in a 50 ml round bottom flask and sonicated for 5 min. The mixture was refluxed at 100 °C under N_2 atmosphere for 4 h after addition of 12.5 mmol of TBHP (2.5 ml). An appropriate time interval, 50 µL of the mixture was taken out from the flask and catalyst was separated from the reaction mixture magnetically. The product was then analyzed using Gas Chromatography (Shimadzu GC-2014) equipped with a capillary column (30 M × 0.25 mm × 0.25 mm) and a FID detector. The reaction was also conducted using commercial TiO_2 and pure CF as catalyst. The conversion and product selectivity were calculated using Eqs. (1) and (2) respectively:

$$\text{Conversion}\,(\%) = \frac{\textit{mole of reactant converted}}{\textit{mole of the reactant in feed}} \times 100 \quad (1)$$

$$\text{Product selectivity}\,(\%) = \frac{\textit{mole of the product formed}}{\textit{mole of the reactant converted}} \times 100 \quad (2)$$

2.3.2 Click Reaction

For synthesis of 1,4-disubstituted 1,2,3-triazoles by 'Click reaction' CuO@mTiO$_2$@CF was used as catalyst. Here, 2-phenyl-2-(4-phenyl-1*H*-1,2,3-triazole-1-yl) ethanol and 2-(4-Phenyl-1*H*-1,2,3-triazol-1-yl) cyclohexanol were synthesized in aqueous medium. In a typical synthesis, in a 25 ml round bottomed flask 1 mmol styrene oxide (0.115 ml) (or, cyclohexene oxide (0.098 ml)), 1.1 mmol sodium azide (72 mg), 1 mmol phenyl acetylene (0.110 ml) and 25 mg of CuO@mTiO$_2$@CF were mixed with 3 ml water. This mixture was then refluxed at 80 °C for 5–6 h with constant stirring. Then the reaction mixture was cooled down to room temperature and the catalyst was separated magnetically. The product was collected by filtration followed by recrystallization.

2.3.3 Biginelli Reaction

We have performed the synthesis of 5-Ethoxycarbonyl-4-phenyl-6-methyl-3,4-dihydropyridin-2(1 *H*)-one and 5-Acetyl-6-methyl-4-phenyl-3,4-dihydropyrimidin-2(1 *H*)-one in solventless condition as representative of Biginelli reaction. In typical synthesis, 1 mmol benzaldehyde (0.101 ml), 1.2 mmol urea (72 mg) and 1 mmol ethyl acetoacetate (0.126 ml) (or acetyl acetone (0.103 ml)) were mixed in a round bottomed flux. To this mixture 25 mg of CuO@mTiO$_2$@CF was added and mixed thoroughly. The reaction mixture was then heated at 80 °C for 1 h. After cooling, the reaction mixture was poured into ice cooled water and catalyst was separated by applying an external magnet. The product was then recrystallized.

2.3.4 Reduction of 4-NP and Trifluralin

To investigate the catalytic activity of CuO@mTiO$_2$@CF towards reduction of nitrophenols, reduction reaction of 4 Nitrophenol (4-NP) was performed in aqueous medium in presence of excess $NaBH_4$. Aqueous solution of 4-NP showed a maximum absorption peak at 317 nm. This peak was immediately red shifted to 400 nm after addition of $NaBH_4$. Successive decrease of this peak (λ_{max} = 400 nm) during reaction and gradual development of a new absorbance peak at 300 nm, characteristic peak of 4-AP indicated the progress of reduction of 4-NP. In a typical run, 4.5 ml 9×10^{-2} mM aqueous solution of 4-NP was mixed with 1 ml of freshly prepared $NaBH_4$ solution (0.2 M). In this solution, 1.5 ml water and 1 ml of aqueous mixture of the catalyst (0.1 gL^{-1}) were added. 4 ml of this reaction mixture was transferred immediately in a quartz cuvette and its absorbance spectra were recorded using an UV–vis spectrophotometer (V-570, Jasco, Japan) at an interval of 1 min. The reaction was carried out at room temperature (30 ± 1 °C). All catalysis reactions were performed in triplicate. We have also performed the reduction of a herbicide (trifluralin) using the same procedure. For reduction of trifluralin, 5 ml of 0.75 mM trifluralin (in 1:1 ethanol), 1 ml (0.2 M) $NaBH_4$, and 2 ml catalyst (0.3 gL^{-1}) were used. Reduction of trifluralin was monitored by observing gradual disappearance of its λ_{max} at 437 nm.

As the initial concentration of $NaBH_4$ was very high, it remained almost constant during the reaction. Hence, it was assumed that rate of the reaction was not dependent on the concentration of $NaBH_4$ and a pseudo first order kinetics with respect to concentration of the 4-NP (or, trifluralin) was applied for the reactions [44–46, 57, 61]. The concentration of the NP (or, trifluralin) in reaction mixture (C_t) was determined from the absorbance of the peak at λ_{max} (λ_{max}(4-NP) = 400 nm, λ_{max}(trifluralin) = 437 nm). The ratio of absorbance of NP (or, trifluralin) A_t (measured at time t) to A_0 (measured at t = 0) is equal to the concentration ratio C_t/C_0 of the NP (or, trifluralin) where, C_0 is the initial concentration of the NP (or, trifluralin). The apparent rate constant (k_{app}) was determined from the following rate equations (3–4):

$$dC_t/dt = -k_{app} \cdot C_t \tag{3}$$

$$\ln\left(C_t/C_0\right) = \ln\left(A_t/A_0\right) = -k_{app} \cdot t \tag{4}$$

The value of k_{app} was calculated from slop of the ln (A_t / A_0) vs. time plot.

2.4 Characterization

Room temperature powder X-ray diffraction (XRD) patterns of the synthesized materials were recorded using a powder X-ray diffractometer (Mini Flex II, Rigaku, Japan) with Cu Kα radiation at a scanning speed of 2°min^{-1}. Field emission scanning electron microscope (FESEM) images and energy dispersive X-ray spectra (EDS) were obtained using Quanta 250 FEG (FEI) and EDAX ELEMENT electron microscope respectively. High resolution transmission electron microscope (HRTEM) images of the samples were obtained using a JEOL JEM 1400, Japan. Room temperature magnetization with respect to an external magnetic field was measured for the synthesized catalysts using a vibrating sample magnetometer (VSM) (EV5, ADE Technology, USA). Multiple point BET surface areas and pore structures were measured with a surface area and porosity analyzer (Micromeritics Tristar 3000, USA). Samples were degassed at 200 °C for ~6 h under N_2 atmosphere before the analysis. Differential scanning calorimetric (DSC) (DSC-60 (Shimadzu, Japan)) analysis were carried out to determine melting point of the products of organic reactions. Infrared spectrophotometer (IRAffinity-1, Shimadzu, Japan)

was used record Fourier transform infrared spectra of the samples. ^{1}H NMR (Nuclear Magnetic Resonance) spectra were recorded on a BRUKER 800 ULTRA SHIELD PLUS (800 MHz) instrument using deuteriated solvent.

3 Results and Discussions

3.1 Structure and Morphology of CuO@mTiO$_2$@CF Nanocomposites

Room temperature powder XRD patterns of synthesized $CoFe_2O_4$, $mTiO_2$@CF and CuO@$mTiO_2$@CF are illustrated in Fig. 1. In the XRD pattern of pure $CoFe_2O_4$ nanopowder (Fig. 1a), the presence of diffraction peaks at 2θ = 18.2°, 30.1°, 35.5°, 37.1°, 43.1°, 53.4°, 56.9° and 62.6° corresponding to the (111), (220), (311), (222), (400), (422), (511), and (440) planes of $CoFe_2O_4$ [JCPDS 22-1086] were observed. For $mTiO_2$@CF (Fig. 1b), presence of peaks at 2θ = 25.3°, 37.8°, 48.1°, 53.9° and 55.06° corresponding to (101), (004), (200), (105) and (211) planes of anatase phase of TiO_2 [JCPDS Card no 21-1272] along with the peaks of $CoFe_2O_4$ confirmed the formation of $mTiO_2$@CF composite. In case of CuO@$mTiO_2$@CF (Fig. 1c, S1), it was observed that, in addition to the peaks of $CoFe_2O_4$ and $mTiO_2$, diffraction peaks at 2θ = 35.48°, 38.66° and 48.08° which correspond to (11−1), (111) and (20−2) planes of CuO [JCPDS Card no 48-1548] respectively were present in the XRD patterns. This confirmed the presence of CuO nanoparticles in the synthesized catalysts.

Figure 2a illustrates the TEM micrograph of the synthesized $CoFe_2O_4$ nanoparticles where average particle was found in the range of ~20–30 nm. In $mTiO_2$@CF a homogeneous mixture of $CoFe_2O_4$ and TiO_2 nanoparticles was observed where particle sizes of CF and TiO_2 were ~25–30 nm and ~15–20 nm respectively (Fig. 2b). In HRTEM micrograph of $mTiO_2$@CF (Fig. 2c) well resolved lattice fringes corresponding to (311) plane of $CoFe_2O_4$ and (101) plane of TiO_2 were observed. TEM micrographs of CuO@$mTiO_2$@CF (Fig. 2d) revealed that CuO nanoparticles (average particle size ~8–10 nm) were deposited homogeneously on the surface of $mTiO_2$@CF nanocomposites. Lattice fringes corresponding to (10−1) plane of CuO, (101) plane of TiO_2 and (311) plane of $CoFe_2O_4$ were also observed in the HRTEM micrograph of CuO@$mTiO_2$@CF (Fig. 2d, S2). FESEM micrograph (Fig. 3a) and elemental mapping of CuO@$mTiO_2$@CF (Fig. 3b–g) also indicated the intimate coexistence of CuO, TiO_2 and CF. From EDS spectra of CuO@$mTiO_2$@CF (Fig. 4), confirmed the presence of its constituents (10 wt% CuO, 67.5 wt% TiO_2, 22.5 wt% CF).

Surface area of as synthesized $mTiO_2$@CF and CuO@$mTiO_2$@CF was obtained by conducting N_2 adsorption desorption isotherm analysis. The isotherms are shown in Fig. 5a. Both the samples showed type IV isotherms of with H1 hysteresis loop indicating their mesoporous nature. However, considerable hysteresis at high relative pressures indicated that the mesopore structure in the samples were not too regular [64]. Pore size distribution of the samples were determined from BJH desorption isotherms and are shown in Fig. 5b. BET surface area and average pore size of $mTiO_2$@CF and CuO@$mTiO_2$@CF were found to be 79.3 m^2/g and 18.3 nm, 58.59 m^2/g and 17.8 nm respectively. Pore volume of $mTiO_2$@CF was decreased from 0.31 to 0.2 cm^3/g with loading of CuO in CuO@$mTiO_2$@CF. This might be due to deposition of CuO nanoparticles within the pores or surface of $mTiO_2$@CF which blocked the pores. Absence of microspores in the samples was confirmed by the t-plots of the samples as extrapolation of straight lines of the t-plots pass through the origin (Fig. 5c) [65]. As the catalyst (CuO@$mTiO_2$@CF) contains mesoporous TiO_2, it is expected that mesoporous nature of TiO_2 will help to absorb the reactant molecules on mesoporous surface of the catalyst and will facilitate the reactions.

VSM was used to measure the room temperature magnetization behaviors of the synthesized catalysts with an applied field of 15,000 Oe and shown in Fig. 6. Saturation magnetization (M_s) and coercivity (H_c) values of pure $CoFe_2O_4$, $mTiO_2$@CF and CuO@$mTiO_2$@CF, was found to be 50.04 emu g^{-1} and 1155 Oe, 12.36 emu g^{-1} and 1092 Oe, 11.12 emu g^{-1} and 1075 Oe respectively. This decrease in the values was quite obvious because the catalyst is composed of magnetic $CoFe_2O_4$ and non-magnetic TiO_2 and CuO nanoparticles.

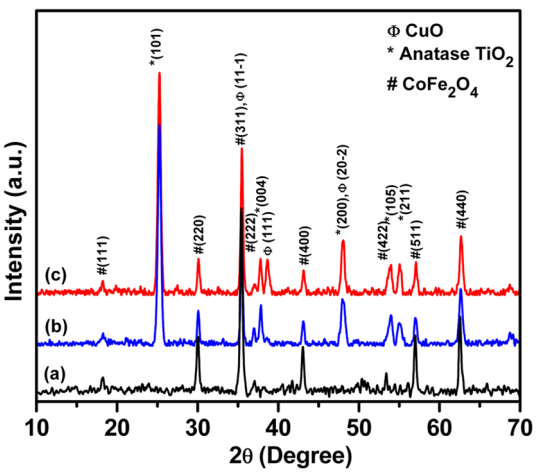

Fig. 1 Room temperature powder XRD patterns of **a** pure CF, **b** $mTiO_2$@CF and **c** CuO@ $mTiO_2$@CF

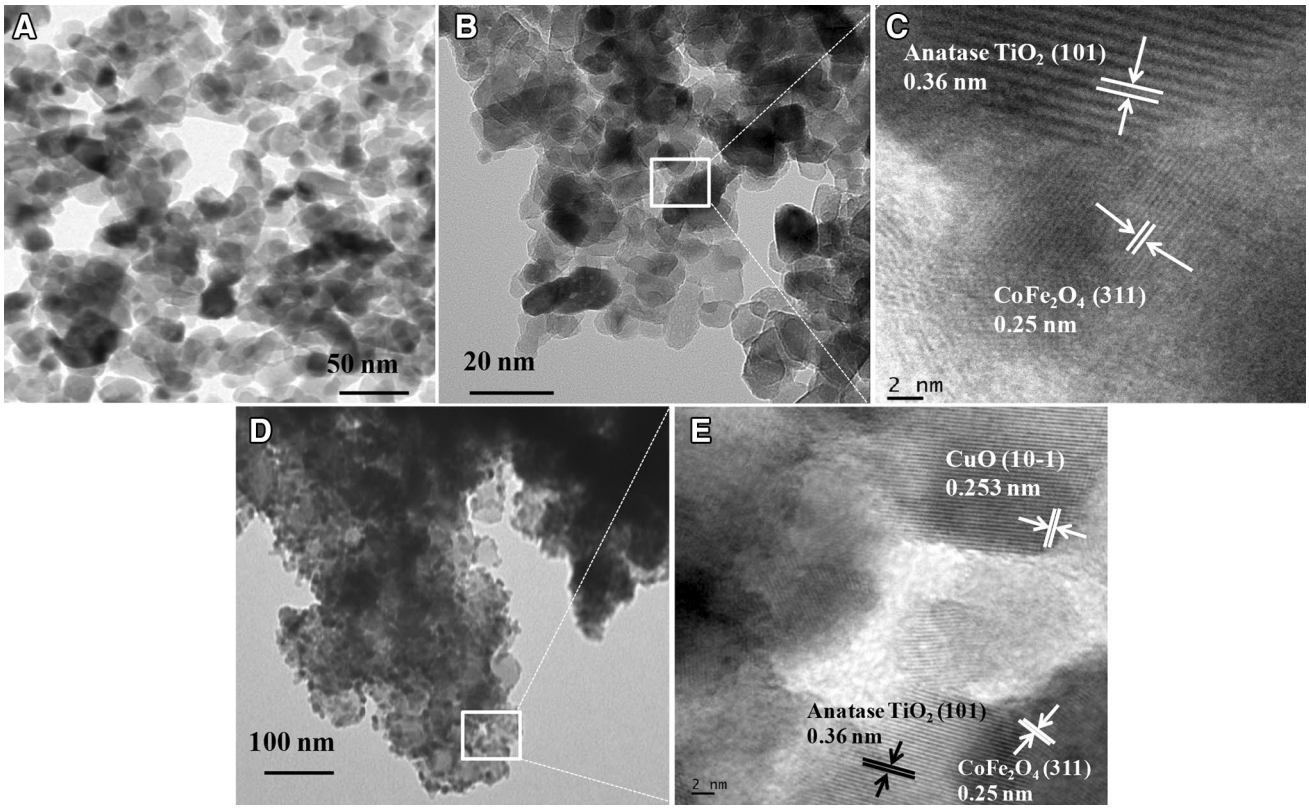

Fig. 2 **a** TEM micrograph of pure CF, **b** $mTiO_2$@CF, **c** HRTEM micrograph of $mTiO_2$@CF, **d** TEM micrograph of CuO@$mTiO_2$@CF, **e** HRTEM micrograph of CuO@$mTiO_2$@CF

3.2 Catalytic Activity of CuO@$mTiO_2$@CF Nanocomposite Towards Epoxidation of Styrene

To investigate the catalytic property of the synthesized catalyst, CuO@$mTiO_2$@CF, selective oxidation reaction of styrene to styrene oxide in presence of TBHP was performed. Qui et al. [66] have reported the use of CuO as catalyst for the conversion of styrene to styrene oxide with 100% conversion of styrene but 45% selectivity. Recently, Ye et al. [14] reported synthesis of CuO@Ag nanowire catalyst for epoxidation reactions. According to Ye et al. though 'free CuO' nanoparticles can produce epoxide upto 80% yield in the first run but it cannot be recycled for further use because of its aggregation. These works indicate that, CuO has the capability to act as catalytically active site in epoxidation reactions. In the present case, it has been observed that, when CuO@$mTiO_2$@CF was used as catalyst for the conversion of styrene to styrene oxide, ~98.5% conversion of styrene (with 77.3% styrene oxide selectivity and 22.7% benzaldehyde selectivity) was achieved within 4 h (Fig. 7 and Fig. S3 (ESI)). The % of conversion of styrene and % of selectivity for styrene oxide achieved by CuO@$mTiO_2$@CF is much higher than previously reported some common catalysts like TS-1, Ti-MCM-41 [67], Mn/Co Salene-MCM-41 [68], CoFeCu(II) salicyladimine-SBA-15 [69] etc.

The epoxidation reaction was also performed in presence of commercial TiO_2 (Hombikat), synthesized TiO_2 ($mTiO_2$), pure $CoFe_2O_4$ (CF), $mTiO_2$@CF and CuO@CF. It was observed that in case of commercial TiO_2 and $mTiO_2$ almost no reaction is occurring. In case of CF, $mTiO_2$@CF and CuO@CF, the conversion of styrene is very poor and ~55% for CF, ~67% for CuO@CF and ~33% for $mTiO_2$@CF even after 10 h of reaction. Though CuO@CF showed ~67% conversion of styrene in the first run but the catalytic activity of the recovered catalysts was decreased in the consecutive reaction cycles. This might be due to the leaching of CuO nanoparticles from CuO@CF. When CuO@$mTiO_2$@CF was used as catalyst, the conversion of styrene was increased significantly (~98.5%) within 4 h of reaction. Therefore, it can be considered that though $mTiO_2$ does not participate in the reaction as active site but provides a porous support to host the catalytically active site (i.e. CuO nanoparticle). The immobilization of CuO nanoparticles within the porous support of $mTiO_2$ helps in two ways (i) it prevents the agglomeration of CuO nanoparticles. Hence

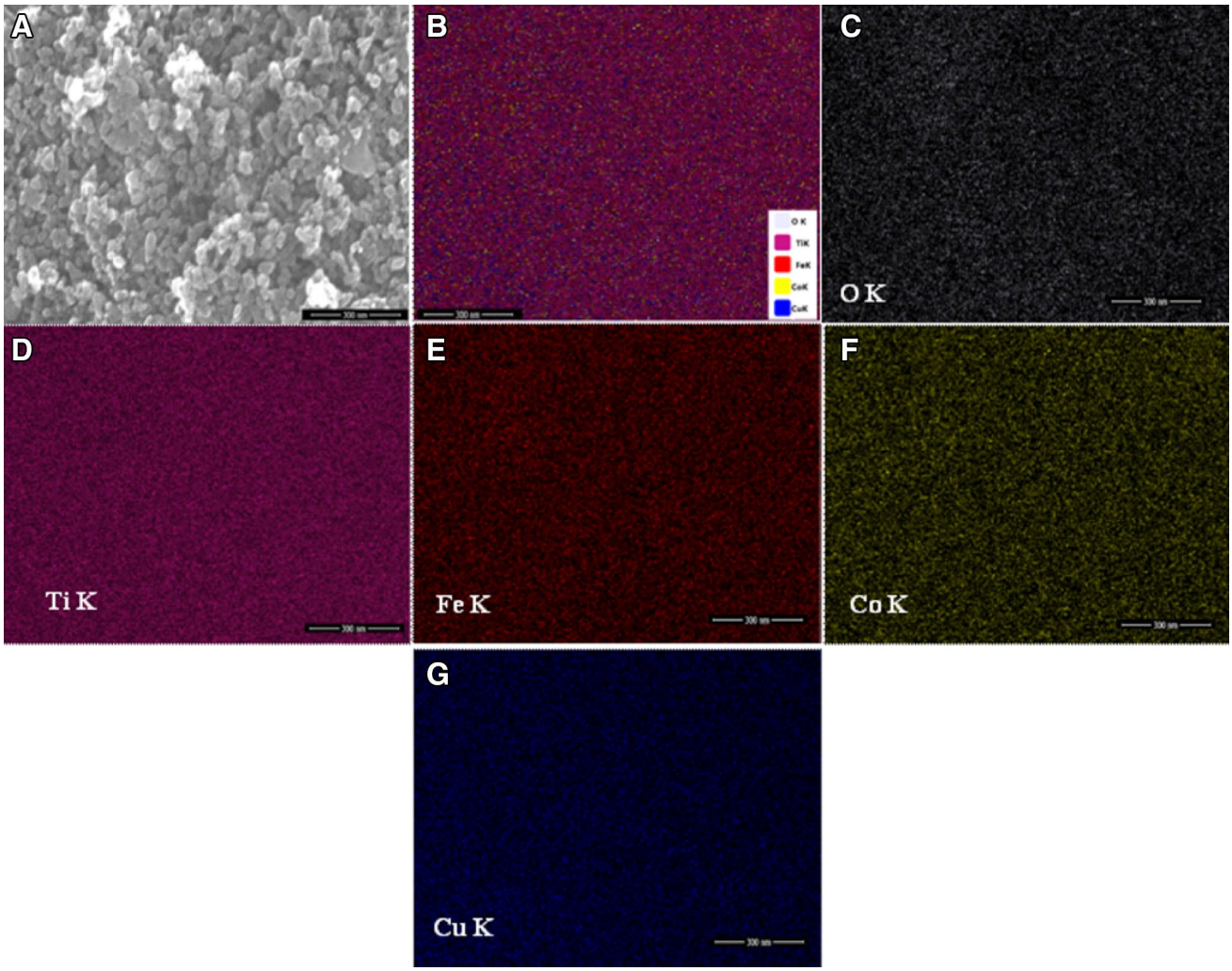

Fig. 3 **a** FESEM micrograph and **b**–**g** Elemental mapping of synthesized CuO@mTiO_2@CF catalyst

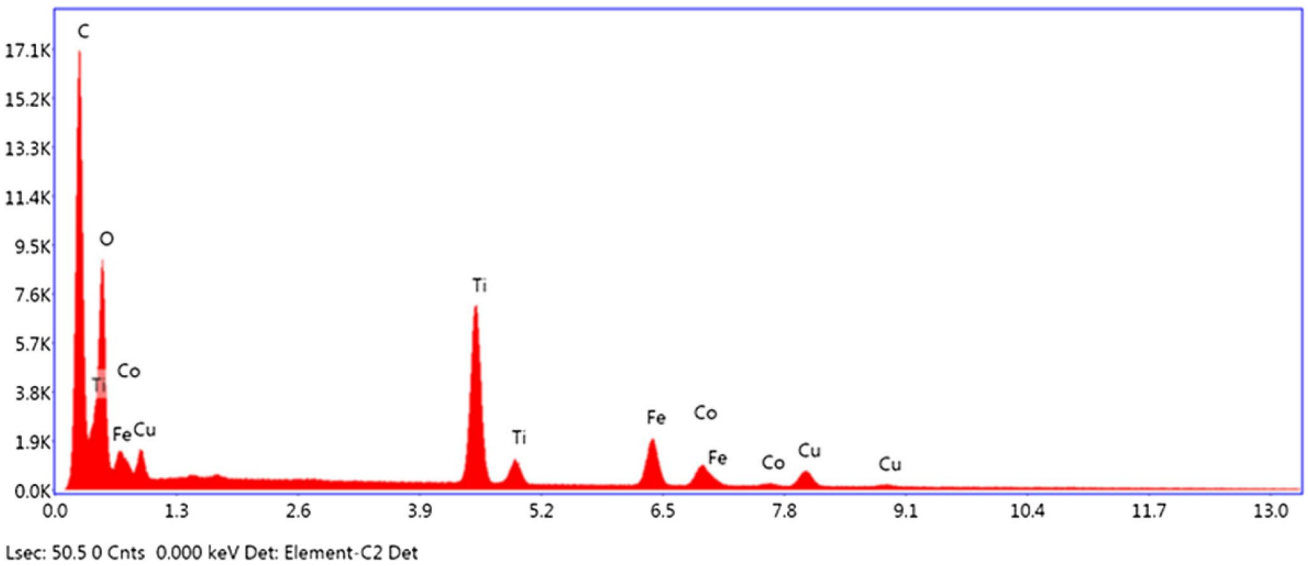

Fig. 4 EDS spectra of synthesized CuO@mTiO_2@CF catalyst

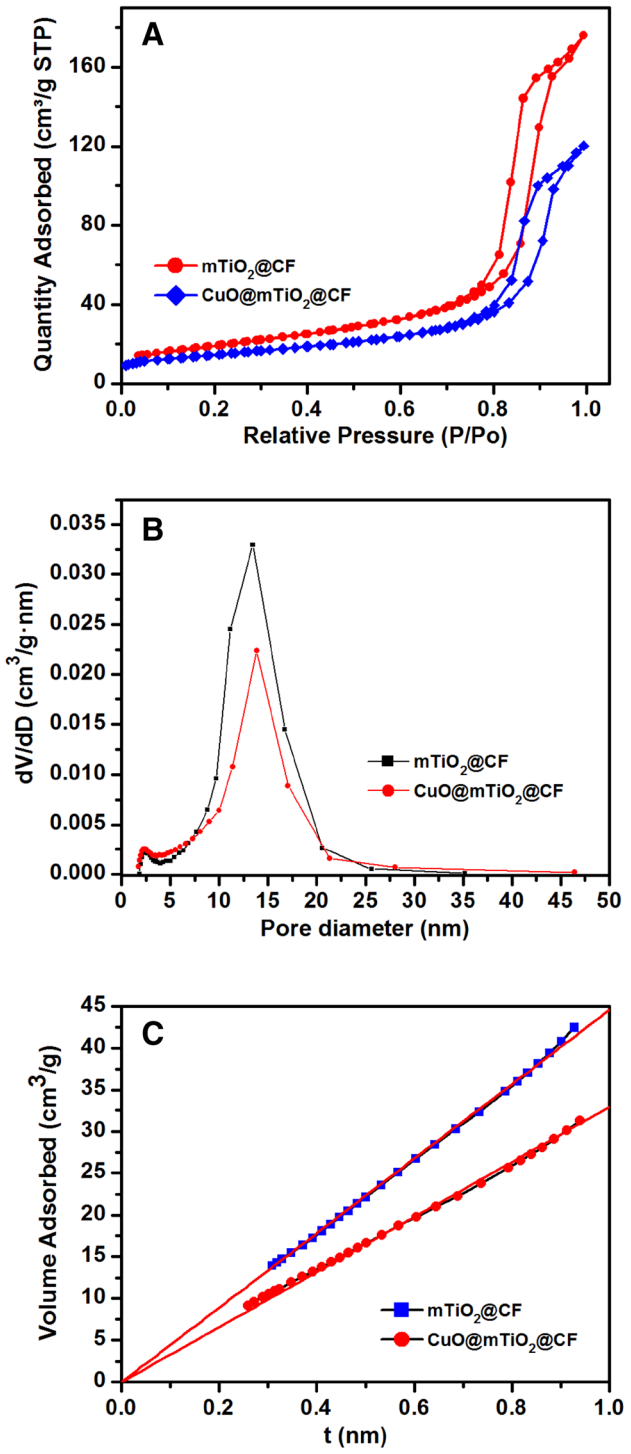

Fig. 5 **a** N_2 adsorption–desorption isotherms, **b** pore size distributions and **c** t-plots of synthesized $mTiO_2$@CF and CuO@$mTiO_2$@CF

the reactant molecules get better accessibility to the catalytically active site. (ii) It also reduces the chance of leaching of CuO nanoparticles during reaction. During CuO@$mTiO_2$@CF catalyzed epoxidation reaction of styrene, CuO helps to activate TBHP molecules by forming metal-oxyl species (intermediate 1). Ultimately styrene oxide formed via an intermediate (intermediate 2) when styrene attacked the intermediate 1 (Scheme 1) [3]. Reaction of two molecules of TBHP leads to the formation of benzaldehyde as by-product (Eq. 5) [3]. It is important to note that, in this the chlorine free process benzaldehyde was obtained as side product, which is also having great industrial value in manufacturing flavors, pharmaceuticals, perfumery etc [3].

As CuO@$mTiO_2$@CF exhibited excellent catalytic activity toward styrene epoxidation reaction, we have performed other reactions, i.e., Click reaction, Biginelli reaction and reduction of 4-nitrophenol and trifluralin by using CuO@$mTiO_2$@CF as catalyst.

3.3 Catalytic Activity of CuO@$mTiO_2$@CF Nanocomposite towards Click Reaction

This catalyst also showed excellent activity for the synthesis of 1,4-disubstituted 1,2,3-triazoles by click reaction. Cyclohexene oxide (or styrene oxide), sodium azide and phenyl acetylene were used as starting materials and water was used as solvent. ~89% yield of 2-phenyl-2-(4-phenyl-1*H*-1,2,3-triazole-1-yl) ethanol and ~87% yield of 2-(4-Phenyl-1*H*-1,2,3-triazol-1-yl) cyclohexanol were observed (Table 1). When these reactions were performed for longer time (12 h), neither increase of yield nor formation of any by-product was obtained. Recently, Jang et al. [29] have reported that, catalytic activity of mesoporous CuO in this type of Click reaction is almost six times higher than that of commercial CuO and ~20 times higher than that of without catalyst when the reaction was performed in aqueous medium. In the present case, CuO nanoparticles of CuO@$mTiO_2$@CF catalyst play a role of bifunctional catalyst. The formation of CuO-azide (to be specific Cu(II)-azide (Intermediate-I)) as catalytically active species helps to activate epoxide and facilitates the delivery of azide during ring opening of epoxide. Simultaneously, another intermediate (Intermediate-II) forms where acetylene coordinates with Cu(II) of CuO@$mTiO_2$@CF catalyst. This intermediate facilitates 1,3-dipolar cycloaddition between –C≡C– bond (intermediate-II) and azide, to produce triazole-CuO@$mTiO_2$@CF complex. Finally the protonolysis

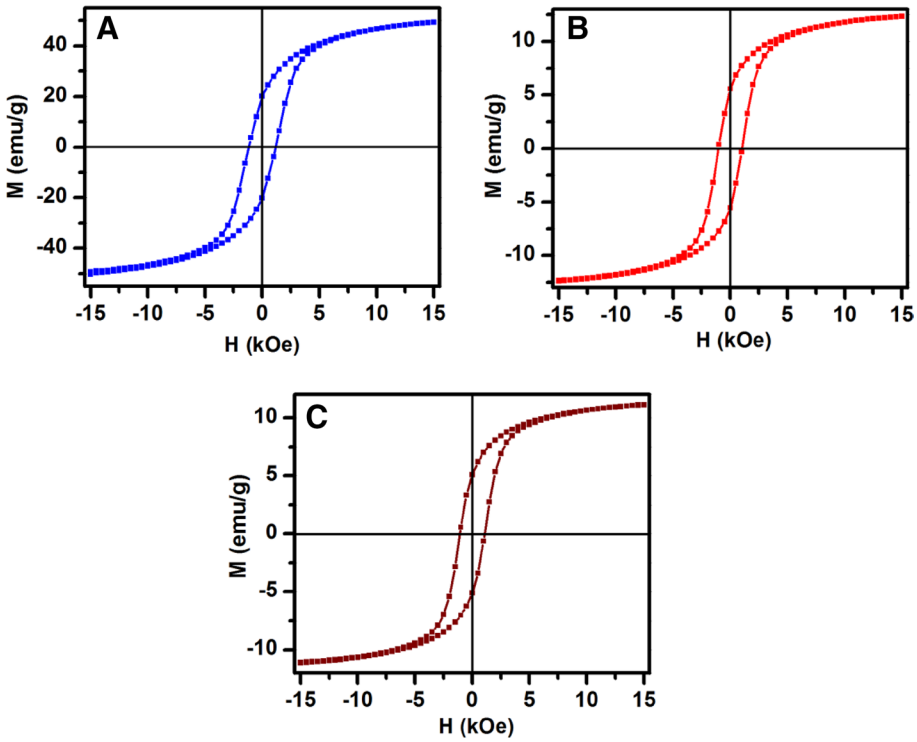

Fig. 6 Magnetic hysteresis loops of **a** CF, **b** $mTiO_2$@CF and **c** CuO@$mTiO_2$@CF

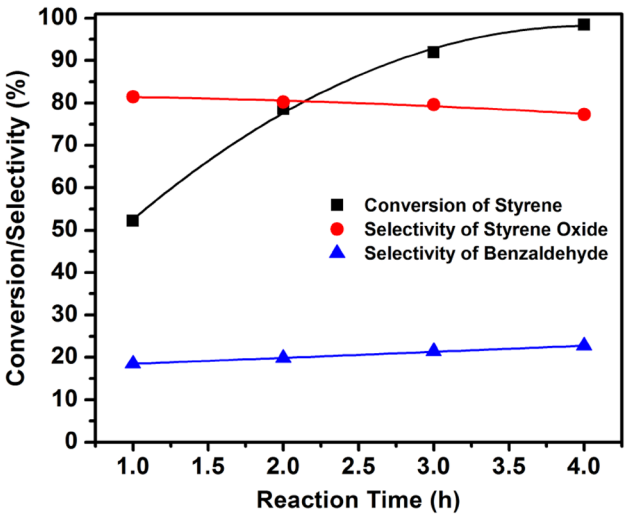

Fig. 7 Change of conversion and product selectivity with time catalyzed by CuO@$mTiO_2$@CF for epoxidation of styrene. Reaction condition: 50 mg catalyst, 5 mmol of styrene and 12.5 mmol of TBHP were stirred in 4 ml of acetonitrile at 100 °C for 4h

of this complex in aqueous medium results the formation of β-hydroxy-1,2,3-triazole compounds [34]. The plausible mechanism of this reaction is shown in Scheme 2.

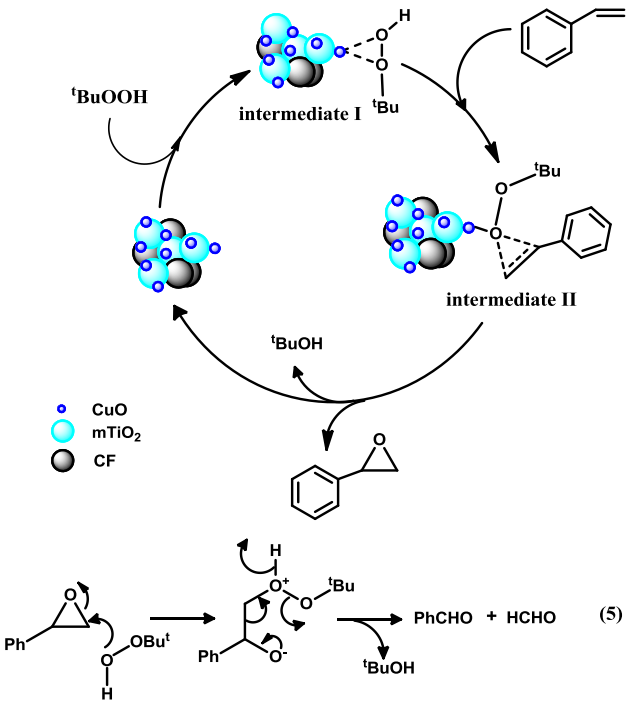

Scheme 1 Plausible mechanism of formation of styrene oxide and benzaldehyde from styrene in presence of TBHP catalyzed by CuO@$mTiO_2$@CF

Table 1 CuO@mTiO$_2$@CF catalyzed synthesis of 1,4-disubstituted 1,2,3-triazoles by 'Click reaction'[a]

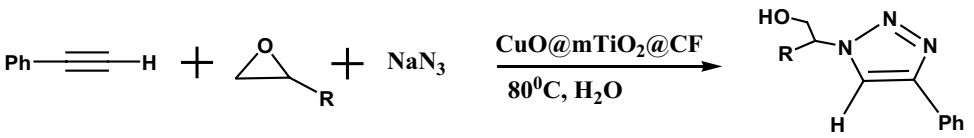

Entry	Epoxide	Product	Reaction time (h)	[b]Yield (%)
1	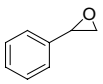	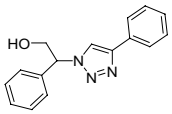	6	89
2		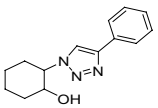	5	87

[a]Reaction conditions: alkyne (1 mmol, 0.110 ml), epoxide (1 mmol (styrene oxide 0.115 ml or, cyclohexene oxide 0.098 ml)), sodium azide (1.1 mmol, 72 mg), CuO@mTiO$_2$@CF (25 mg), water (3 ml), reaction temperature 80 °C

[b]Isolated yield

3.4 Catalytic Activity of CuO@mTiO$_2$@CF Nanocomposite Towards Biginelli Reaction

To determine the activity of synthesized catalyst (CuO@mTiO$_2$@CF), towards Biginelli reaction, the reactions between benzaldehyde, ethyl acetoacetate (or, acetyl acetone) and urea were performed as model reactions in presence of CuO@mTiO$_2$@CF under solventless condition. The results are summarized in Table 2. ~96% yield of 5-Ethoxycarbonyl-4-phenyl-6-methyl-3,4-dihydropyridin-2(1 *H*)-one and ~92% yield of 5-Acetyl-6-methyl-4-phenyl-3,4-dihydropyrimidin-2(1 *H*)-one were observed. Performing these reactions for longer duration (6 h) did not affect the % of yield or formation of any other product. The role of CuO nanoparticles in the synthesized catalyst is to increase the electrophilicity of carbonyl carbons of both aldehyde and ethyl acetoacetate (or acetyl acetone) via formation of a coordination complex type intermediate (Intermediate-I).Then aldol-type condensation between aldehyde and 1,3-diketone leads to the formation of Intermediate-II. Furthermore, N donor site of Urea also coordinates with CuO nanoparticles, which activated it for 1,4 addition reaction. This reacted with aldol type intermediate to generate ureides, which ultimately cyclized to Biginelli product (scheme 3) [19].

^{1}HNMR, FTIR and melting point determination of the synthesized compounds were used to identify the products obtained from Biginelli reaction and Click reaction. DSC has been used to determine the melting point of the synthesized organic molecules because the sharp endothermic point in the DSC scan indicates the melting point of the compound. The data obtained from ^{1}HNMR, FTIR and DSC were matched with the existing literature and confirmed the formation of the product. Details of spectral data of the synthesized compounds obtained from Styrene epoxidation reaction, Biginelli reaction and Click reaction are provided in supplementary information (Figs. S3–S15, supplementary information).

3.5 Catalytic Activity of CuO@mTiO$_2$@CF Nanocomposite Towards Reduction of 4-NP and Trifluralin

To investigate the applicability of CuO@mTiO$_2$@CF as catalyst towards reduction of nitrophenols, the reduction reaction of 4-NP in presence of excess $NaBH_4$ was studied. It was observed that, time required for complete reduction of 4-NP was 5 min (Fig. 8). The rate of the reaction was 0.72 min^{-1} which is comparable or in some cases higher than the reported values when various other catalysts were used [44–48, 51–59, 61]. The mechanism of this type of reduction reaction is well established [44–46, 49, 51, 52, 55, 57, 61]. The catalytic reduction reaction occurred via relaying of electrons from the BH_4^- donor to the acceptor 4-NP. First, 4-NP and $NaBH_4$ were absorbed on the surface of the catalyst. The hydrogen atoms, which were formed from BH_4^- after electron transfer (ET) to the CuO nanoparticles attacked 4-NP molecules to reduce them.

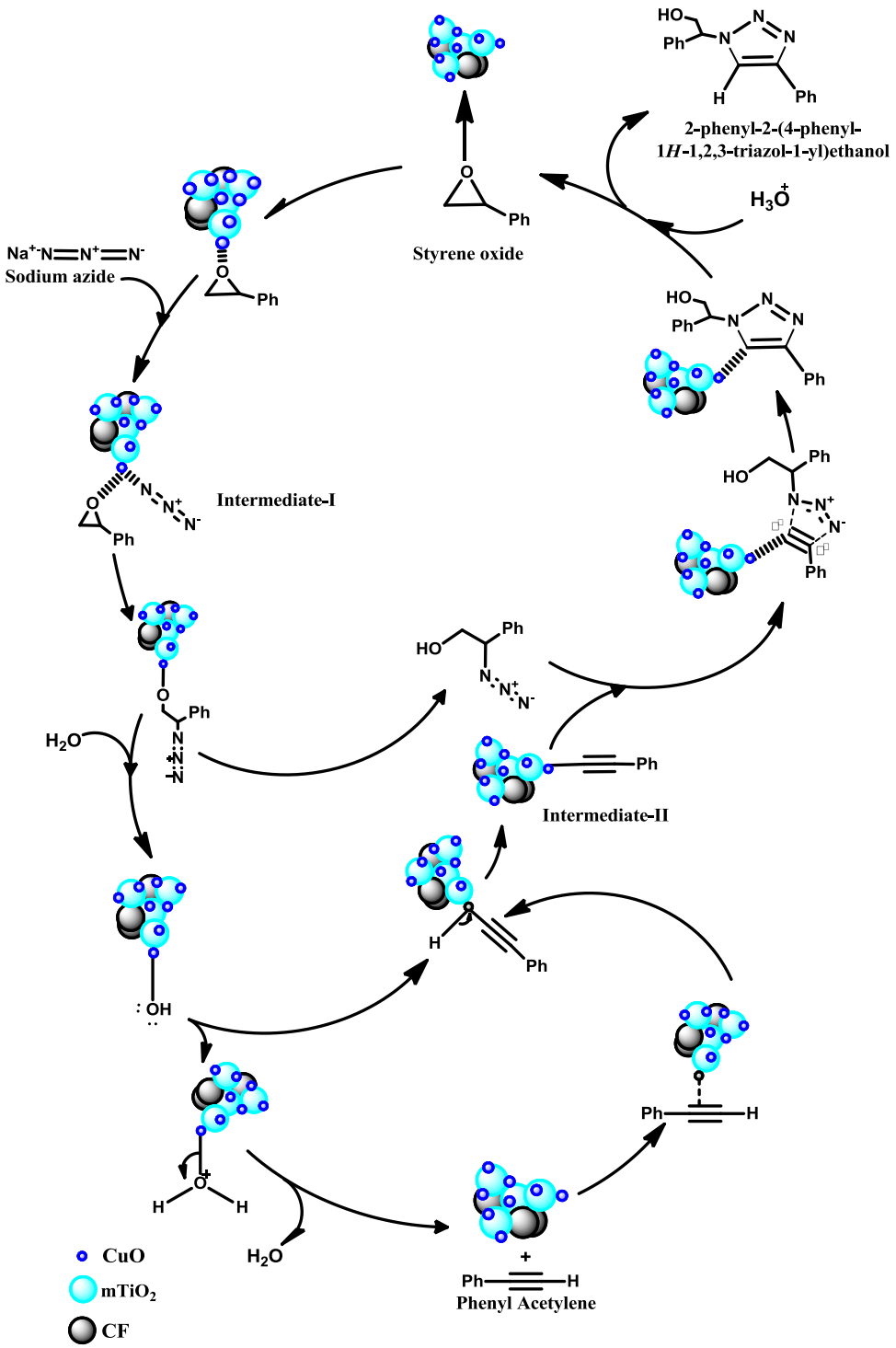

Scheme 2 Plausible reaction mechanism involved in Click reaction catalyzed by CuO@mTiO_2@CF catalyst for synthesis of 1,4-disubstituted 1,2,3-triazoles

Inspired by the high catalytic efficiency of CuO@ mTiO_2@CF towards reduction of 4-NP, we investigated the decolorization of trifluralin via reduction of its -NO_2 groups. Trifluralin is a highly toxic herbicide, which is used in various countries to control variety of annual grass and broadleaf weed species. But, it remains in water as

Table 2 CuO@mTiO$_2$@CF catalyzed synthesis of 3,4-dihydro-pyrimidin-2(1 H)-ones a by Biginelli reaction[a]

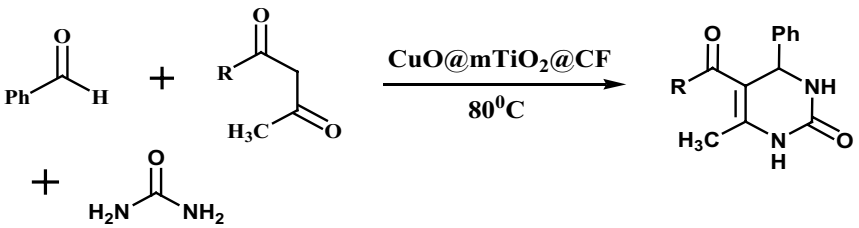

Entry	R	Product	Reaction time (h)	[b]Yield(%)
1	OEt	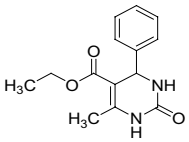	1	96
2	CH_3	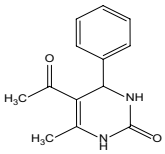	1	92

[a]Reaction Conditions: Benzaldehyde (1 mmol, 0.101 ml), Urea (1.2 mmol, 72 mg), 1,3-Diketone (1 mmol, 0.126 ml ethyl acetoacetate or 0.103 ml acetylacetone), CuO@mTiO$_2$@CF (25 mg), Solventless condition, reaction temperature 80 °C

[b]Isolated yield

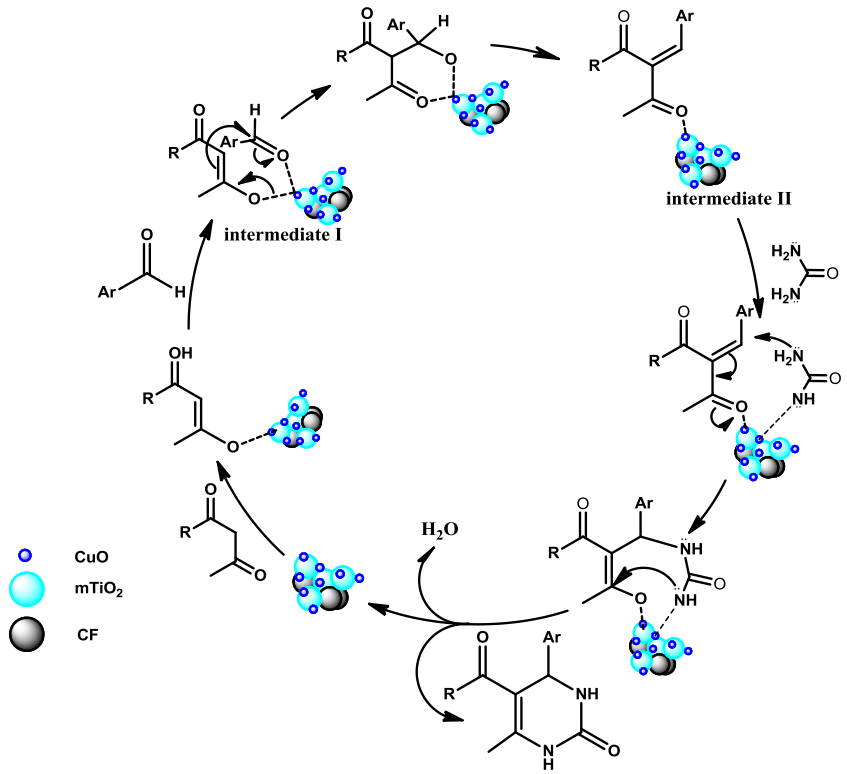

Scheme 3 Plausible mechanism involved in Biginelli reaction catalyzed by CuO@mTiO$_2$@CF catalyst in the synthesis of 3,4-dihydropyrimidinone

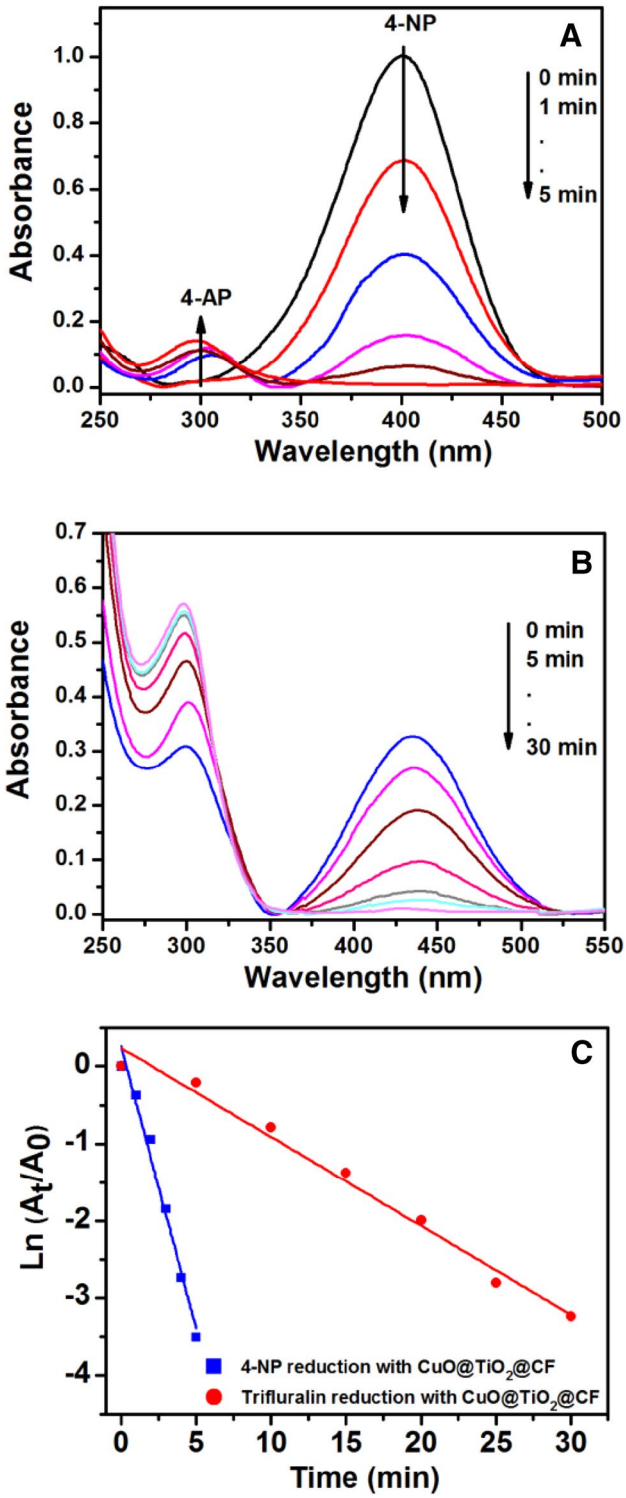

Fig. 8 Time dependent UV–Vis spectral changes of the reaction mixtures of **a** 4-NP, **b** Trifluralin and $NaBH_4$ catalyzed by CuO@$mTiO_2$@CF, **c** pseudo first kinetic plot of 4-NP and Trifluralin reduction catalyzed by CuO@$mTiO_2$@CF

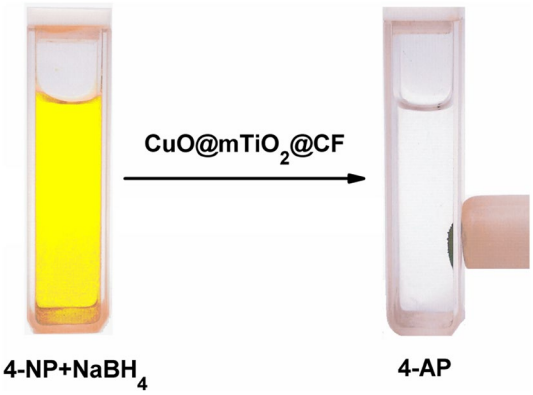

Fig. 9 Reduction of 4-NP in presence of $NaBH_4$ and CuO@$mTiO_2$@CF catalyst and Magnetic separation of CuO@$mTiO_2$@CF catalyst by applying a magnet externally after completion of reaction

pesticide residue and causes severe water pollution. It was observed that CuO@$mTiO_2$@CF can efficiently reduce trifluralin in presence of excess $NaBH_4$ (Fig. 8). The rate of the reaction was 0.11 min^{-1}.

3.6 Reusability of Magnetically Separable CuO@$mTiO_2$@CF Catalyst After Catalysis Reactions

As CuO@$mTiO_2$@CF catalyst possesses magnetic character, it can be easily separated from the reaction mixture after completion of the reaction by using an external magnet (Fig. 9). After completion of all the reaction the catalyst was separated magnetically from the reaction mixture, washed several times by distilled water and dried at 100 °C for 12 h. The reusability of the synthesized catalyst was also tested for all the reactions. No considerable loss of activity of the catalyst was observed after 5th reuse (Fig. 10). TEM and FESEM micrographs and XRD patterns (Fig. 11) of the recycled catalysts revealed that the crystal structure and morphology of the catalyst remained same after 5th cycle of catalysis reaction. These results thus clearly demonstrated stability and homogeneity of the synthesized catalyst.

4 Conclusions

In the present study, CuO loaded $mTiO_2$@CF nanocatalyst was successfully synthesized by employing a simple chemical methodology. The synthesized catalyst showed its high efficiency in various organic reactions namely, (i) epoxidation of styrene in presence of TBHP, (ii) synthesis

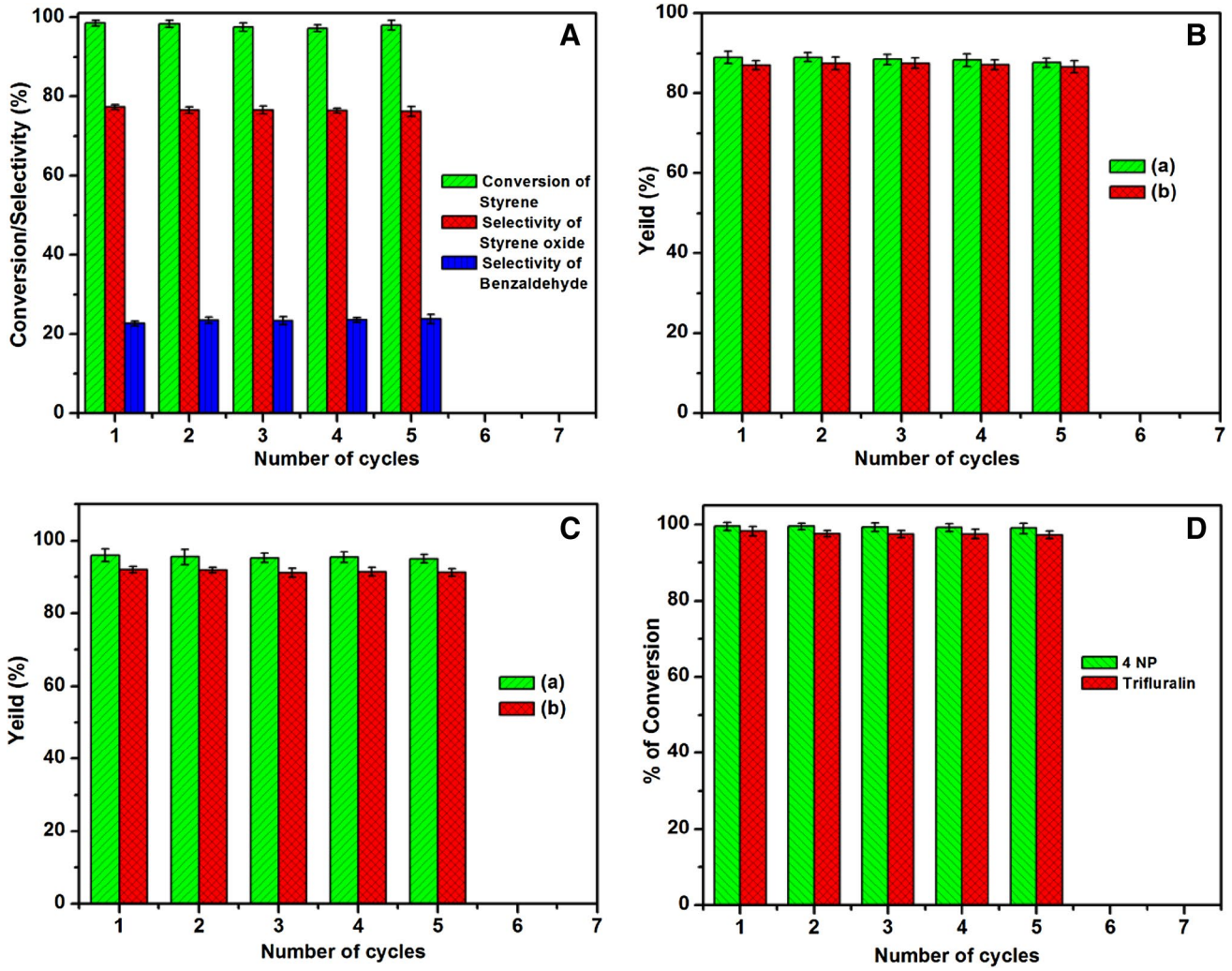

Fig. 10 Reusability of CuO@mTiO$_2$@CF for **a** conversion of styrene, selectivity of styrene oxide and benzaldehyde, **b** synthesis of (**a**) 2-phenyl-2-(4-phenyl-1*H*-1,2,3-triazole-1-yl) ethanol and (**b**) 2-(4-Phenyl-1*H*-1,2,3-triazol-1-yl) cyclohexanol via Click reaction, **c** synthesis of (**a**) 5-Ethoxycarbonyl-4-phenyl-6-methyl-3,4-dihydropyridin-2(1*H*)-one and **b** 5-Acetyl-6-methyl-4-phenyl-3,4-dihydropyrimidin-2(1*H*)-one via Biginelli reaction and **d** conversion of 4-NP to 4-AP

of DHPMs using Biginelli reaction under solventless condition, (iii) synthesis 1,2,3 triazoles by 'click reaction' in aqueous medium and (iv) reduction of 4-NP and a herbicide trifluralin in presence of excess $NaBH_4$. Moreover, magnetic separation offered by the synthesized catalyst, helped to overcome the separation problem associated with pure nanosized catalysts. Additionally, the catalyst can also be reused for several times without any decrease of its activity. To the best of our knowledge, we are reporting simple a method for the preparation of a CuO, mesoporous TiO_2 and $CoFe_2O_4$ based catalyst for the first time, which exhibited high catalytic efficiency for above mentioned four types of important reactions as well as demonstrated its easy magnetic separation from reaction mixtures and its reusability. The usefulness of CuO@mTiO$_2$@CF as catalyst for various important organic reactions, its high catalytic efficiency, easy separation and good reusability make it an attractive nanocatalyst.

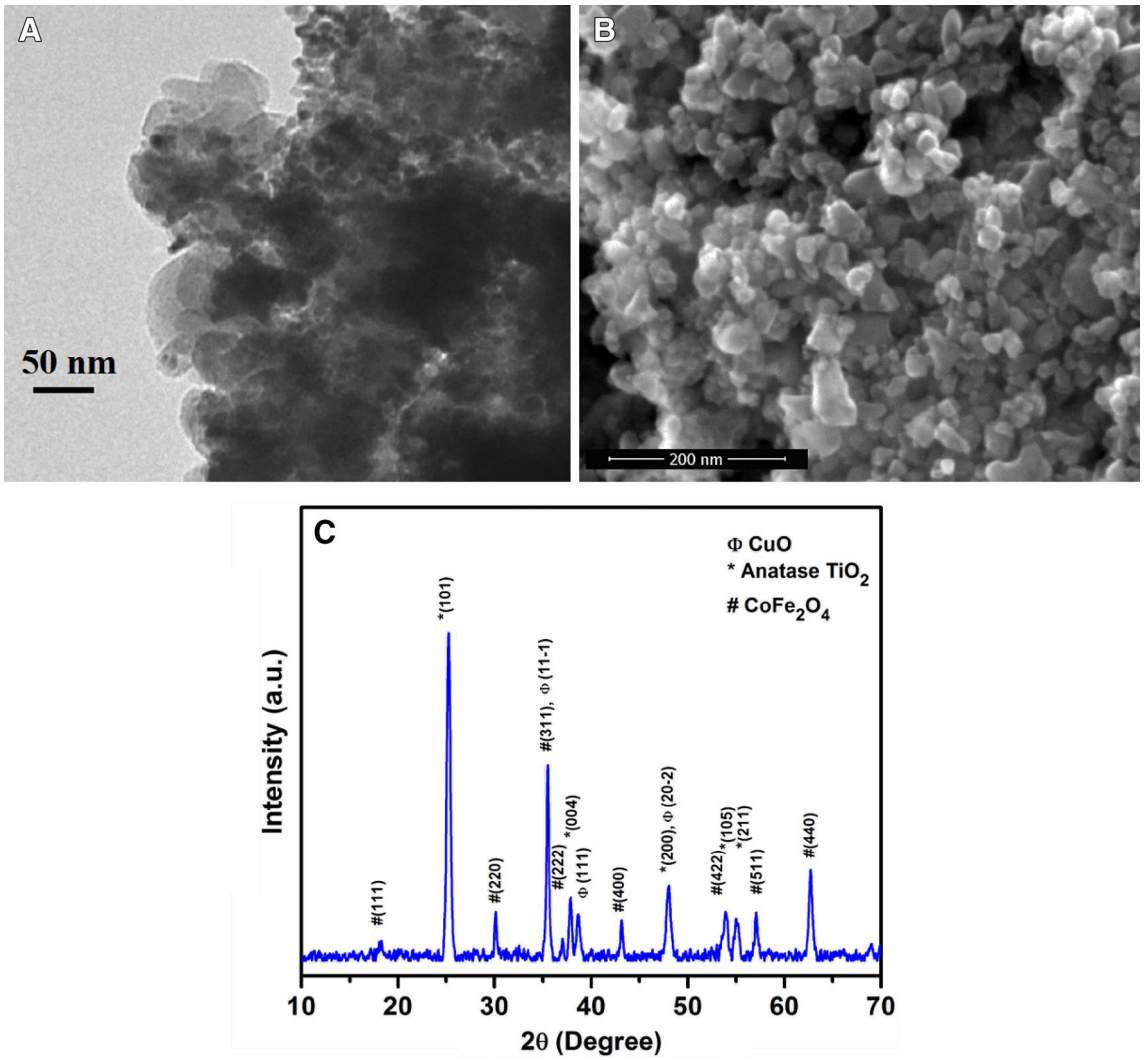

Fig. 11 **a** TEM, **b** FESEM image **c** XRD pattern of the recycled CuO@mTiO_2@CF catalyst

Acknowledgements Dr. N. N. Ghosh gratefully acknowledges financial support from CSIR, India (CSIR Sanction letter No. 02(147)/13/EMR-II). We also express our thanks to Prof. Paul A. Millner, Mr Martin Fuller, University of Leeds, UK and Prof. Sabu Thomas, Mahatma Gandhi University, India for recording TEM micrographs.

References

1. Linares N, Canlas CP, Garcia-Martinez J, Pinnavaia TJ (2014) Catal Commun 44:50–53
2. Shehzad A, Panneerselvam S, Linow M, Bocola M, Roccatano D, Mueller-Dieckmann J, Wilmanns M, Schwaneberg U (2013) Chem Commun 49:4694
3. Wang A, Jing H (2014) Dalton Trans 43:1011
4. Choudhary VR, Dumbre DK, Patil NS, Uphade BS, Bhargava SK (2013) J Catal 300:217.
5. Freyschlag CG, Madix RJ (2011) Mater Today 14:134.
6. Liu Y, Tsunoyama H, Akita T, Tsukuda T (2010) Chem Commun 46:550
7. Balu AM, Hidalgo JM, Campelo JM, Luna D, Luque R, Marinas JM, Romero AA (2008) J Mol Catal A 293:17
8. Zhang X, Wang G, Yang M, Luan Y, Dong W, Dang R, Gao H, Yu J (2014) Catal Sci Tech 4:3082.
9. Wang F, Liu C, Liu G, Liu J (2015) J Porous Mater 22:1423
10. Liu J, Wang F, Qi S, Gu Z, Wu G (2013) New J Chem 37:769
11. Liu J, Wang F, Xu T, Gu Z (2010) Catal Lett 134:51
12. Yang D, Yang N, Ge J (2013) Cryst Eng Comm 15:7230
13. Zhang D-H, Li G-D, Li J-X, Chen J-S (2008) Chem Commun 3414.
14. Ye Z, Hu L, Jiang J, Tang J, Cao X, Gu H (2012) Catal Sci Technol 2:1146.
15. Thao NT, Huyen LTK (2015) Chem Eng J 279:840.
16. Jain S.L, Singhal S, Sain B (2007) Green Chem 9:740.
17. Javidi J, Esmaeilpour M, Dodeji FN (2015) RSC Adv 5:308.
18. Oliverio M, Costanzo P, Nardi M, Rivalta I, Procopio A (2014) ACS Sustainable. Chem Eng 2:1228
19. Mondal J, Sen T, Bhaumik A (2012) Dalton Trans 41:6173

20. Safari J, Gandomi-Ravandi S (2013) J Mol Catal A 373:72
21. Zhu A, Li Q, Li L, Wang J (2013) Catal Lett 143:463
22. Zamani F, Izadi E (2013) Catal Commun 42:104
23. Rajack A, Yuvaraju K, Praveen C, Murthy Y (2013) J Mol Catal A 370:197
24. Tamaddon F, Moradi S (2013) J Mol Catal A 370:117
25. Kour G, Gupta M, Paul S, Gupta RVK (2014) J Mol Catal A 392:260
26. Prakash GKS, Lau H, Panja C, Bychinskaya I, Ganesh SK, Zaro B, Mathew T, Olah GA (2014) Catal Lett 144:2012
27. Kolb HC, Finn MG, Sharpless KB (2001) Angew Chem Int Ed 40:2004
28. Prasad AN, Thirupathi B, Raju G, Srinivas R, Reddy BM (2012) Catal Sci Technol 2:1264.
29. Jang S, Sa YJ, Joo SH, Park KH (2016) Catal Commun 81:24
30. Boningari T, Olmos A, Reddy BM, Sommer J, Pale P (2010) Eur J Org Chem 33:6338
31. Sharghi H, Ebrahimpourmoghaddam S, Doroodmand MM, Purkhosrow (2012) Asian J Org Chem 1:377
32. Kumar BSPA, Reddy KHV, Madhav B, Ramesh K, Nageswar YVD (2012) Tetrahedron Lett 53:4595
33. Kumaraswamy G, Ankamma K, Pitchaiah A (2007) J Org Chem 72:9822
34. Naeimi H, Nejadshafiee V (2014) New J Chem 38:5429
35. Alonso F, Moglie Y, Radivoy G, Yus M (2011) J Org Chem 76:8394
36. Díez-González S, Stevens ED, Nolan SP (2008) Chem Commun 4747.
37. Yadav JS, Reddy BVS, Reddy GM, Chary DN (2007) Tetrahedron Lett 48:8773
38. Wan L, Cai C (2012) Catal Lett 142:1134
39. Tavassoli M, Isfahani AL, Moghadam M, Tangestaninejad S, Mirkhani V, Baltork IM (2015) Appl Catal A 503:186
40. Hu H, Xin JH, Hu H, Wang X, Miao D, Liu Y (2015) J Mater Chem A 3:11157
41. Patel R, Suresh S (2006) J Hazard Mater 137:1729
42. Wang Z-Z, Zhai S-R, Zhai B, An QD (2015) Eur J Inorg Chem 1692.
43. Vaidya MJ, Kulkarni SM, Chaudhari RV (2003) Org Process Res Dev 7:202.
44. Ghosh BK, Hazra S, Naik B, Ghosh NN (2015) Powder Technol 269:371
45. Ghosh BK, Hazra S, Ghosh NN (2016) Catal Commun 80:44
46. Naik B, Hazra S, Prasad VS, Ghosh NN (2011) Catal Commun 12:1104
47. El-Bahy ZM (2013) Appl Catal, A 468:175.
48. Lv J-J, Wang A-J, Ma X, Xiang R-Y, Chen J-R, Feng J-J (2015) J Mater Chem A 3:290
49. Lin F-h, Doong R-a (2014) Appl Catal, A 486:32.
50. Noh J-H, Meijboom R (2015) Appl Catal A 497:107.
51. Sharma G, Jeevanandam P (2013) Eur J Inorg Chem 6126.
52. Shin KS, Cho YK, Choi J-Y, Kim K (2012) Appl Catal A 413–414:170–175.
53. Chang Y-C, Chen D-H (2009) J Hazard Mater 165:664
54. Chi Y, Yuan Q, Li Y, Tu J, Zhao L, Li N, Li X (2012) J Colloid Interface Sci 383:96
55. Zheng J, Dong Y, Wang W, Ma Y, Hu J, Chen X, Chen X (2013) Nanoscale 5:4894
56. Kalarivalappil V, Divya CM, Wunderlich W, Pillai SC, Hinder SJ, Nageri M, Kumar V, Vijayan BK (2016) Catal Lett 146:474
57. Naik B, Hazra S, Desagani D, Ghosh BK, Patra MK, Vadera SR, Ghosh NN (2015) RSC Adv 5:40193.
58. Tang M, Zhang S, Li X, Pang X, Qiu H (2014) Mater. Chem Phys 148:639
59. Feng J, Su L, Ma Y, Ren C, Guo Q, Chen X (2013) Chem Eng J 221:16.
60. Nasrollahzadeh M, Atarod M, Sajadi SM (2016) Appl Surf Sci 364:636
61. Moitra D, Ghosh BK, Chandel M, Jani RK, Patra MK, Vadera SR, Ghosh NN (2016) RSC Adv 6:14090.
62. Hasan Z, Cho D-W, Chon C-M, Yoon K, Song H (2016) Chem Eng J 298:183.
63. Rajput AB, Hazra S, Ghosh NN (2013) J Exp Nanosci 8:629.
64. Peng T, Zhao D, Dai K, Shi W, Hirao K (2005) J Phys Chem B 109:4947
65. Naik B, Prasad V, Ghosh NN (2010) J Porous Mater 17:115
66. Qiu G, Dharmarathna S, Zhang Y, Opembe N, Huang H, Suib SL (2012) J Phys Chem C 116:468
67. van der Waal JC, van Bekkum H (1997) J Mol Catal A 124:137
68. Luo Y, Lin J (2005) Microporous Mesoporous Mater 86:23
69. Yang Y, Hao S, Qiu P, Shang F, Ding W, Kan Q (2010) Reac Kinet Mech Catal 100:363